frontiers in Marine Science

ORIGINAL RESEARCH
published: 09 July 2021
doi: 10.3389/fmars.2021.657762

Genetic Recombination of the Mantle Color Pattern of Two Boring Giant Clam (*Tridacna crocea*) Strains

Junjie Wang[1†], Zihua Zhou[2,3,4,5†], Haitao Ma[2,3,4,5], Jun Li[2,3,4,5], Yanping Qin[2,3,4,5], Jinkuan Wei[2,3,4,5], Xingyou Li[2,3,4,5], Qingliang Liao[2,3,4,5], Yunqing Li[2,3,4,5], Gongpengyang Shi[2,3,4,5], Yinyin Zhou[2,3,4,5], Yuehuan Zhang[2,3,4,5] and Ziniu Yu[2,3,4,5*]*

[1] Guangdong Provincial Key Laboratory for Healthy and Safe Aquaculture, Guangdong Provincial Engineering Technology Research Center for Environmentally-Friendly Aquaculture, Guangzhou Key Laboratory of Subtropical Biodiversity and Biomonitoring, School of Life Sciences, South China Normal University, Guangzhou, China, [2] Key Laboratory of Tropical Marine Bio-resources and Ecology, Guangdong Provincial Key Laboratory of Applied Marine Biology, South China Sea Institute of Oceanology, Innovation Academy of South China Sea Ecology and Environmental Engineering, Chinese Academy of Sciences, Guangzhou, China, [3] Southern Marine Science and Engineering Guangdong Laboratory (Guangzhou), Guangzhou, China, [4] University of the Chinese Academy of Sciences, Beijing, China, [5] Hainan Provincial Key Laboratory of Tropical Marine Biology Technology, Sanya Institute of Oceanology, Chinese Academy of Sciences, Sanya, China

OPEN ACCESS

Edited by:
Xiaotong Wang,
Ludong University, China

Reviewed by:
Liqiang Zhao,
Guangdong Ocean University, China
Karsoon Tan,
Shantou University, China

***Correspondence:**
Yuehuan Zhang
yhzhang@scsio.ac.cn
Ziniu Yu
carlzyu@scsio.ac.cn

[†] These authors have contributed equally to this work

Specialty section:
This article was submitted to Aquatic Physiology, a section of the journal Frontiers in Marine Science

Received: *23 January 2021*
Accepted: *03 June 2021*
Published: *09 July 2021*

Citation:
Wang J, Zhou Z, Ma H, Li J, Qin Y, Wei J, Li X, Liao Q, Li Y, Shi G, Zhou Y, Zhang Y and Yu Z (2021) Genetic Recombination of the Mantle Color Pattern of Two Boring Giant Clam (Tridacna crocea) Strains. Front. Mar. Sci. 8:657762. doi: 10.3389/fmars.2021.657762

According to the RGB law display, the polymorphism of the giant clam mantle color pattern is through four iridocytes. The boring giant clam (*Tridacna crocea*) exhibits diverse mantle colors, including blue, green, purple, gold, and orange. In order to evaluate the genetic laws driving these mantle color patterns, a complete diallel cross between two color strains [blue strain (only blue iridocyte) and the yellow-green strain (yellow and green iridocytes)] was performed. Using a single-to-single mating system, two intra-strain crosses (BB and YY) and two reciprocal inter-strain crosses (BY and YB) were produced in triplicates. Higher fertilization rate and hatching rate were observed in all experimental groups, suggesting that there was no sperm–egg recognition barrier between the two strains. In the grow-out stage, the size of the reciprocal hybrids was larger than that of the two pure strains with a degree of heterosis. In addition, compared with the two pure strains, the hybrids have higher larval metamorphosis rate and higher survival rate. At 1 year of age, the mantle color pattern of pure strains showed 100% stable inheritance, while the reciprocal hybrids exhibited colorful patterns (a combination of blue, yellow, and green), suggesting that there was a genetic recombination of the mantle colors during the stable expression period. These results provide a theoretical basis for the formation of the mantle color of giant clam and its genetic segregation law, as well as provide guidance for genetic breeding of giant clams.

Keywords: *Tridacna crocea*, the boring giant clam, crossbreeding, mantle color's pattern, genetic recombination

INTRODUCTION

Throughout nature, biophotonic structures have evolved sophisticated arrangements of pigments and structural reflectors that can manipulate light in animal skin, cuticle, feathers, and fur (Mäthger et al., 2013). These colors are found in a variety of animal taxonomy, from diminutive marine copepods to terrestrial insects and birds, and have attracted great research interest in recent

years. Recent studies on biophotonic structures focuses on the characterization of nanostructures responsible for iridescence and the behavioral function of iridescent colors (Kinoshita and Yoshioka, 2005; Cuthill et al., 2017).

Recently, scientists have discovered that the mantle color of giant clams is the result of structural color, which is aroused by a display of different iridocytes according to the RGB law display (Ozog, 2009; Todd et al., 2009; Holt et al., 2014; Rossbach et al., 2020; Long et al., 2021). During the photosymbiotic process of giant clams, the forward scattering of iridocytes illuminates the internal zooxanthellae deeper inside the mantle, and the backward reflection produces the unique color of the giant clam mantle (Ghoshal et al., 2016). Although the giant clam iridocytes distributed in the mantle have been well studied, little is known about the genetic basis or pattern of mantle color inheritance (Kim et al., 2017; Mies, 2019). Scientists have observed that giant clam strains with blue and yellow-green color patterns can be stably inherited, and there are phenotypic differences between the two color strains (Zhou et al., 2020). However, it is unclear whether the mantle color pattern is segregated or genetically recombined with the pigmentation of the shells during natural replenishment process.

The iridophores in the mantle of the giant clams are composed of iridocytes, which contain stacks of regularly arranged platelets of uniform thickness (Griffiths et al., 1992). These platelets form a crystal lattice, which produces maximum light interference at wavelengths of about 400 nm or slightly higher than 400 nm. Interference may extend the reflected light into the blue and green parts of the visible spectrum (Griffiths et al., 1992; Neo et al., 2015; Rossbach et al., 2020). Iridocytes can be divided into four types (red, yellow, green, and blue) and can be expressed as one, two, or more types in a single individual (Ghoshal et al., 2016). Blue, yellow, and green iridocytes are common, while red iridocytes are rare (Zhou et al., 2020). In our study, we examined the blue strain (blue iridocytes) and kelly strain (green and yellow iridocytes) of the boring giant clams.

In order to determine the genetic law of the reciprocal hybrids between two mantle color patterns of boring giant clams, complete diallel crosses were carried out in triplicate using a single-to-single mating system. The fertilization, survival, metamorphosis, and growth of progenies of each group during the larval, nursery, and grow-out phases were compared. In this study, the use of inter-strain hybridization technique clearly revealed the occurrence and genetic laws of the mantle coloration of reciprocal hybrids. The findings of this study can provide guidance for the genetic breeding of giant clams.

MATERIALS AND METHODS

Broodstock Collection and Spawning

Sexually matured boring giant clams used as broodstock in this study were collected from Huangyan Island (East of Zhongsha Islands) (N 15.160812, E 117.760336) in the South China Sea. The clams were held in an insulated container filled with seawater and transported by boat to the Hainan Tropical Marine Life Experimental Station at the Chinese Academy of Sciences. Thirty parent clams from each of two mantle color strains (blue and yellow-green) were selected from the Huangyan Island population. The average shell length (SL) and total weight of the blue strain were 80.30 ± 7.96 mm and 165.32 ± 45.69 g, respectively, whereas the average SL and total weight of yellow-green clams were 89.53 ± 7.48 mm and 230.44 ± 72.56 g, respectively. The broodstock of these two strains was held separately in 2,000-L raceways and provided with gentle aeration and continuous flow of sand-filtered seawater from Sanya Bay, Hainan Island.

When these broodstocks from the two strains mature, they were induced to spawn by exposure to air for 10 min, followed by a temperature shock from 27.0 to 30.0°C. Once spawning was initiated, the individuals were placed separately in 5-L plastic beakers filled with seawater (30.0°C) and closely observed to collect uncontaminated eggs or sperm. Since Tridacninae is a simultaneous hermaphrodite animal (Braley et al., 2018), it is necessary to carefully collect sperm and eggs separately from each clam separately. If clams simultaneously release eggs and sperm, the eggs and sperm will be removed from the experiment. The collected sperm was filtered through a 25-μm mesh to ensure that there are no eggs. The collected eggs were set aside for at least 30 min before being inspected using a microscope. The eggs were discarded if fertilized. In total, the eggs or sperm of 18 individuals from each population were used in this study.

Cross-Fertilization

Four progenies, i.e., BB (B♀ × B♂), BY (B♀ × Y♂), YB (Y♀ × B♂), and YY (Y♀ × Y♂), were produced by factorial hybridization between the blue (B) and yellow-green strain (Y) clams. The fertilized eggs of each progeny were divided equally and placed into two 5-L beakers. A small number of fertilized eggs were sampled to evaluate the success rate of fertilization and the survival of D-stage larvae. The remaining fertilized eggs were suspended in a 100-L tank with a density of 30–40 eggs/ml for incubation. The water temperature and salinity were maintained at 28.6–29.7°C and 32 ppt, respectively. The entire experiment was repeated three times using three groups of broodstock, with each group consisting of one male and female blue and yellow-green stains (**Table 1**).

TABLE 1 | Experimental design for the crossbreeding of the boring giant clam between the blue and yellow-green strains.

Parents	B_1♂	Y_1♂	B_2♂	Y_2♂	B_3♂	Y_3♂
B_1♀	BB_1	BY_1	—	—	—	—
Y_1♀	YB_1	YY_1	—	—	—	—
B_2♀	—	—	BB_2	BY_2	—	—
Y_2♀	—	—	YB_2	YY_2	—	—
B_3♀	—	—	—	—	BB_3	BY_3
Y_3♀	—	—	—	—	YB_3	YY_3

BB and YY indicate blue and yellow-green strain's progeny, respectively. BY and YB indicate reciprocal hybrids between blue and yellow-green strains, respectively. The subscript number 1, 2, 3 denotes three replicates, and each replicate was conducted by single pair mating. Each replicate consisted of single sperm from one clam and single eggs from other clam of each strain.

Larval and Juvenile Rearing

Thirty hours after fertilization, D-stage larvae of each cohort (BB, BY, YB, and YY) were collected using a 60-μm sieve and maintained separately in 1,000-L tanks. The initial larval density was adjusted to 2 larvae/ml and maintained at this level by controlling the water volume. In the first 5 days, the larvae were fed with *Isochrysis galbana* at a density of 3,000 cells/ml/day. From the sixth to eight day, they were immersed in seawater containing symbiotic algae (zooxanthellae) at a density of 30 cells/ml for 2 h per day. The outdoor larval rearing tanks was equipped with gentle aeration, transparent polycarbonate roof sheeting, and a 50% light transmittance shade-cloth, of which reduced the daily-maximum photosynthetically active radiation (PAR) from 0 to 572.6 μmol/s/m^2 [Dataflow Systems Pty Ltd. (Christchurch, New Zealand) light logger] (Braley et al., 2018; Militz et al., 2017, 2019). The water temperature and salinity were maintained at 28.5–29.7°C and 32 ppt, respectively.

Most larvae (≥90%) attached and developed secondary shells, feet, gills, and symbiotic system. They reached the juvenile stage on the 20th day. No substrate was used during the spat nursing stage. Larvae settle within 7 days, and then the newly settled spats were transferred to 1,000-L tanks filled with sand-filtered seawater, with maintained gentle aeration, water flow, and 50% natural lighting for 10 weeks. When the SL reached 3–5 mm, the spats were transferred to coral stone substrate and kept in 1,000-L tanks for another 4 weeks. When the SL of spat reached 8–10 mm, they were transferred to an artificial raceway system with continuous circulating water until they reach 1 year old. The water temperature and salinity were maintained at 25.7 to 30.2°C and 32 ppt, respectively.

Sampling and Measurements

The hatching index (cleaved rate and D-stage larva rate), survival rate (at days 7, 15, 90, and 360), and growth (egg diameter, D-stage larvae size, and spat size on the same day) of each group were determined following the method of Zhou et al. (2020). The survival rate on day 7 and day 15 was defined as the ratio of the number of individuals at different developmental stages to the number of D-stage larvae. The survival rate on day 90 and day 360 was defined as the ratio of the number of individuals at different stages to the number of spat on day 30.

On day 90, spats (SL approx. 3–5 mm) of each of the three replicates in each group (BB, YY, BY, and YB) were divided equally into 40 substrates (coral stone 16–18 cm in diameter) with a density of 30 individuals/substrate. In other words, there were 3,600 spats on 120 substrates for each group, and 14,400 spats on 480 substrates in the entire experiment. The substrates were cleaned monthly, dead clams were removed, and the density of each group was readjusted to maintain similar levels among the groups. As the spat grew, the density was reduced from 30 individuals/substrate to 15 individuals/substrate.

Spectroscopic Microscopy

Mantle iridocyte samples among each group were imaged and determined by microspectrophotometry under a Zeiss AxioObserver D1M inverted microscope (Carl Zeiss AG, Oberkochen, Germany) equipped with a broadband halogen lamp (providing ample light in the measured range of 400–700 nm) that provided illumination. For spectroscopy, a small region of the sample (∼1-μm diameter) was imaged on the entrance slit (0.2 mm width) of the imaging spectrometer (Horiba JobinYvon iHR320; Horiba Group, Kyoto, Japan), with light entering the spectrometer dispersed horizontally by a grating (150 lines/mm, blazed for 500 nm). The resulting image was captured with a thermoelectrically cooled silicon charge-coupled device (Horiba JobinYvon Synapse detector) using an integration time of 0.05 s. The spectrum was obtained from an area less than a single iridocyte and normalized to a calibrated specular reflectivity standard (Ocean Optics STAN-SSH) for analyses. The 50 × objective was a Zeiss EC EpiPlan-NEOFLUAR lens with a numerical aperture of 0.8 and 3.8-μm depth of field. Other details of microspectrophotometer and analytical methods are as previously described in Ghoshal et al. (2016).

Statistical Analysis

Two-way analysis of variance (Fisher's) was used for multiple comparisons to analyze the differences of the average hatching index, survival rate, and growth parameters among groups. In order to improve the normality and homoscedasticity, prior to analysis, the hatching rate and survival rate were arcsine-transformed, and the growth parameters were logarithmically transformed (base 10). All statistical analyses were performed using SPSS 23.0. $p < 0.05$ was considered statistically significant for all tests, unless noted otherwise.

Mid-parental heterosis (H) was analyzed to evaluate the potential application of hybrids in aquaculture in the first year using the following formula (Zhang et al., 2007, 2017; Wang et al., 2011; Wang and Côté, 2012):

$$H(\%) = [X_{F1} - (X_{BB} + X_{YY})/2] \times 100/[(X_{BB} + X_{YY})/2]$$

where X_{F1} represents the mean phenotypic value (SL, survival rate, etc.) of the reciprocal hybrids, while X_{BB} and X_{YY} represent the mean phenotypic value (SL, survival rate, etc.) of the blue and yellow-green strain progenies on the same day, respectively.

In order to determine the effects of egg origin (B vs. Y) and mating strategies (homozygous vs. heterozygous crosses) on the survival and growth of clams, a two-factor analysis of variance was used (Cruz and Ibarra, 1997; Zhang et al., 2007, 2017), as follows:

$$Y_{ijk} = \mu + EO_i + MS_j + (EO \times MS)_{ij} + e_{ijk}.$$

Here, Y_{ijk} is the mean SL, wet weight, or survival rate of k replicate from the i egg origin, and the j is the mating strategy. EO_i is the effect of egg origin on SL (survival rate) (i = 1, 2). MS_j is the effect of mating strategy on SL (survival rate) (j = 1, 2). $(EO \times MS)_{ij}$ is the interaction effect between the egg origin and mating strategy, while e_{ijk} is the random observation error (k = 1, 2, 3).

Single-parent heterosis is the improved performance over the purebred offspring of the maternal strain, calculated using the following formula (You et al., 2015; Zhang et al., 2017, 2020b):

$$I_{BY}(\%) = (X_{BY} - X_{BB})/X_{BB} \times 100$$

$$I_{YB}(\%) = (X_{YB} - X_{YY})/X_{YY} \times 100$$

where I_{BY} and I_{YB} indicate single-parent heterosis for the BY and YB offspring, respectively. X_{BB}, X_{YY}, X_{BY}, and X_{YB} indicate the mean phenotypic value (SL, survival rate, etc.) of BB, YY, BY, and YB, respectively.

RESULTS

Hatching Rate

There was no significant difference in the mean egg size between the blue strain (94.84 ± 2.53 μm) and yellow-green strain (95.30 ± 1.09 μm) ($p > 0.05$) (**Table 2**). Highly cleaved rates (>90%) were observed among all four groups, suggesting that there were no sperm–egg recognition barriers between the two strains. The D-stage larva rate of the YY group (81.26 ± 15.77%) was significantly lower ($p < 0.05$) than that of the other three groups, which was mainly affected by both mating strategies and egg origin.

Survival Rate

On day 7, the mean survival rate of larvae in all four groups exceeded 90%, but the survival rate of the BY group was lower than that of other three groups. The heterosis of larval survival rate was −2.21%, and the single heterosis of the BY and YB progenies were −2.25 and −2.18%, respectively. The survival rate of larvae was affected by egg origin (**Tables 2**, **3**). On day 15, the metamorphosis rates of BB (31.87 ± 10.57%) and BY (37.28 ± 16.84%) were significantly higher ($p < 0.05$) than those of YY (8.69 ± 5.81%) and YB (16.83 ± 10.48%). Mid-parental heterosis was 33.41%, and the single heterosis of the BY and YB groups were 16.98 and 93.67%, respectively. The rate of metamorphosis was primarily affected by egg origin (**Tables 2**, **3**).

On day 90, the survival rates of progeny of all four groups were over 85%. The survival rates of the BY (94.61 ± 9.17%) and YB (90.45 ± 5.80%) progenies were significantly higher ($p < 0.05$) than those of the BB (85.10 ± 9.47%) and YY (87.72 ± 7.40%) progenies. Mid-parental heterosis was 3.86%, and the single heterosis of the BY and YB groups were 3.08 and 4.60%, respectively. The survival rate of spat was mainly affected by the interaction of egg origin and mating strategies (**Tables 2**, **3**). On day 360, the survival rates of all four groups exceeded 80%, with the survival rates of reciprocal hybrids being slightly higher ($p > 0.05$) than those of the two pure strains. The mid-parental heterosis for survival was 3.37%, and the single heterosis of the BY and YB groups were 1.15 and 5.64%, respectively. The survival rate of giant clam spats was also affected by the interaction of egg origin and mating strategies (**Tables 2**, **3**).

Growth Rate

Thirty hours after fertilization, the size of D-stage larvae of the BY group was smaller than that of the other three groups without a significant difference, showing obvious effects of mating strategies (**Tables 3**, **4**). At the end of the planktonic stage, the SL of the BB group was the largest among the four groups with a significant difference, which was affected by the maternal effect (**Tables 3**, **4**). On day 15, the SL of BY (257.33 ± 55.48 μm) and YB (230.38 ± 53.18 μm) was significantly larger ($p < 0.05$) than that of BB (215.03 ± 40.02 μm) and YY (203.70 ± 17.66 μm). The mid-parental heterosis was 16.47%, and the single heterosis of the BY and YB groups were 19.67 and 13.10%, respectively (**Table 4**).

On day 90, the SL of reciprocal hybrid progeny was significantly larger ($p < 0.05$) than that of pure strains, showing the interaction effect of egg origin and mating strategies (**Tables 3**, **4**). The mid-parental heterosis was 10.18%, and the single heterosis of the BY and YB groups were 9.86% and 10.50%, respectively (**Table 4**). On day 360, SL of BB (37.86 mm) was significantly smaller ($p < 0.05$) than that of other three groups (40.83–45.46 mm), which was affected by the interaction between egg origin and mating strategies (**Tables 3**, **4**). The mid-parental heterosis was 12.35%, and the single heterosis of the BY and YB groups were 13.44 and 11.34%, respectively (**Table 4**).

Coloration

At 1 year of age, the mantle color of the BB progeny was 100% blue, and the blue iridocytes have a light absorption peak at 475 nm. The mantle color of the YY progeny was 100% yellow-green, and the yellow-green iridocytes have a light absorption peak range from 550 to 650 nm (**Table 5** and **Figures 1**, **2**). In contrast, the BY and YB progenies both showed mixed colors, including blue, yellow, and green colors. These iridocytes of all hybrids have two peaks at 475 and 550–650 nm (**Table 5** and **Figures 1**, **2**). In other words, the mantle color patterns of the reciprocal hybrids displayed genetic recombination, which can be defined as a phenomenon of the common dominant expression derived from two strains' parents.

DISCUSSION

Performance Traits

Fertilization rate is a key parameter used to evaluate the commercial production potential of crossbreeding progeny (You et al., 2015). Our study demonstrates that using one of the mantle color strain as a sperm donor (two-way fertilization) can achieve a higher fertilization rate and hatching rate, which indicates that there is no reproductive isolation between blue and yellow-green mantle color strains (Zhou et al., 2020; Zhang et al., 2021).

Zhou et al. (2021) previously investigated the growth difference between blue and yellow-green mantle color strains of boring giant clams and concluded that in wild populations, the yellow-green broodstock is always larger than the blue broodstock. Generally, the heterosis of a crossbreed between two particular strains depends on the square of the difference in gene frequency between strains. If the crossed strains have no difference in gene frequency, there will be no heterosis, while

TABLE 2 | Hatching index, survival ability and metamorphism of two strain's progeny (BB and YY) and their reciprocal hybrids (BY and YB), as well as heterosis (*H* and *I*).

Items	Hatching index			Survival rate (%)			
	Egg diameter (μ m)	Cleaved rate (%)	D-stage (%)	Day 7	Day15	Day 90	Day 360
BB	94.84 ± 2.53a	97.96% ± 10.66%a	90.76% ± 9.83a	93.70 ± 7.45a	31.87 ± 10.57a	85.10 ± 9.47b	82.03 ± 1.62a
YY	95.30 ± 1.09a	98.08% ± 1.87%a	81.26 ± 15.77b	95.48 ± 3.52a	8.69 ± 5.81b	87.72 ± 7.40b	80.24 ± 2.85a
BY	−−	98.47% ± 0.98%a	92.82 ± 6.03a	91.59 ± 2.78a	37.28 ± 16.84a	94.61 ± 9.17a	82.97 ± 3.55a
YB	−−	98.44% ± 0.97%a	90.16 ± 7.38a	93.40 ± 3.21a	16.83 ± 10.48b	90.45 ± 5.80a	84.77 ± 3.27a
H(%)	−−	0.44	6.37	−2.21	33.41	3.86	3.37
I_{BY}(%)	−−	0.52	2.27	−2.25	16.98	3.08	1.15
I_{YB}(%)	−−	0.37	10.95	−2.18	93.67	4.60	5.64

$\bar{X}$ ± SD indicates mean ± standard deviation. H indicates mid-parent heterosis; and I_{BY} and I_{YB} indicate the single parent heterosis of BY and YB groups, respectively. For cleavage rate, D-stage rate, cumulative survival on different days, n = 9 (3 replicates × 3) in each experimental group. Different superscript letters in each column indicate significant difference (p<0.05).

TABLE 3 | Analysis of variance (ANOVA) showing the egg origin (EO) and mating strategy (MS) effects for survival and growth of each experimental group at different time points.

Items	Source	*df*	Survival rate			Shell length		
			MS	***F-value***	***p***	***MS***	***F-value***	***p***
Day7	EO	1	0.013	4.144	0.050	0.001	4.357	0.038*
	MS	1	0.086	0.649	0.426	<0.0001	2.959	0.086
	EO × MS	1	0.002	0.105	0.748	0.001	5.008	0.026*
Day 15	EO	1	0.469	31.245	<0.0001***	0.178	31.204	<0.0001***
	MS	1	0.047	3.114	0.087	0.451	79.118	<0.0001***
	EO × MS	1	0.001	0.072	0.790	0.001	0.235	0.628
Day 90	EO	1	0.024	1.795	0.191	0.036	3.559	0.060
	MS	1	0.025	1.874	0.182	0.055	5.346	0.021*
	EO × MS	1	0.139	10.429	0.003**	0.410	40.02	<0.001***
Day360	EO	1	0.025	3.108	0.87	0.001	0.109	0.741
	MS	1	0.027	3.276	0.080	0.053	8.359	0.004**
	EO × MS	1	0.017	2.106	0.047*	0.005	0.750	0.387

**indicates p<0.05; **indicates p<0.01; ***indicates p<0.001.*

TABLE 4 | Growth index of of two strain's progeny (BB and YY) and their reciprocal hybrids (BY and YB), at different days post-fertilization, as well as heterosis (*H* and *I*).

Items	D larvae (μ m)	Day 7 (μ m)	Day 15 (μ m)	Day 90 (mm)	Day 360 (mm)
BB	151.87 ± 3.51a	182.81 ± 4.96a	215.03 ± 40.02b	4.93 ± 1.53b	37.86 ± 5.30c
YY	151.81 ± 3.55a	180.50 ± 2.45b	203.70 ± 17.66b	4.81 ± 1.35b	40.83 ± 5.61b
BY	150.56 ± 3.38a	180.78 ± 6.42b	257.33 ± 55.48a	5.35 ± 0.98a	42.95 ± 5.05ab
YB	152.95 ± 5.21a	180.82 ± 5.01b	230.38 ± 53.18a	5.32 ± 1.53a	45.46 ± 5.02a
H(%)	0.21	−0.47	16.47	9.55	12.35
I_{BY}(%)	−0.86	−1.11	19.67	8.52	13.44
I_{YB}(%)	1.29	0.18	13.10	10.60	11.34

H indicates mid-parent heterosis; and I_{BY} and I_{YB} indicate the single parent heterosis of BY and YB groups, respectively. For growth traits (SL, WW), n = 90 (3 replicates × 30) in each experimental group. Different superscript letters in each column indicate significant differences (p < 0.05).

when one allele is fixed in one strain and the other allele is fixed in another strain, the heterosis will be the greatest (Zhang et al., 2007; Wang et al., 2011; Wang and Côté, 2012; Ma et al., 2021). In our study, the size of the reciprocal hybrids was larger than the progenies of the two pure strains during the grow-out stage, and these hybrids obviously have heterosis with a simple epistatic effect. Since differently colored iridocytes in the mantle have different solar utilization efficiencies, they caused growth differences between the two pure strains and the reciprocal hybrids (Holt et al., 2014).

As an aquaculture animal, the viability of the boring giant clam is a very important performance trait, and it is known to be

TABLE 5 | Mantle coloration pattern of two strain's progeny (BB and YY), and their reciprocal hybrids (BY and YB).

Items	Blue type	Yellow type	Mixing type	Total
BB	100 (100%)	0	0	100 (100%)
YY	0	100 (100%)	0	100 (100%)
BY	0	0	100 (100%)	100 (100%)
YB	0	0	100 (100%)	100 (100%)

Mixing type includes the blue and yellow-green colors.

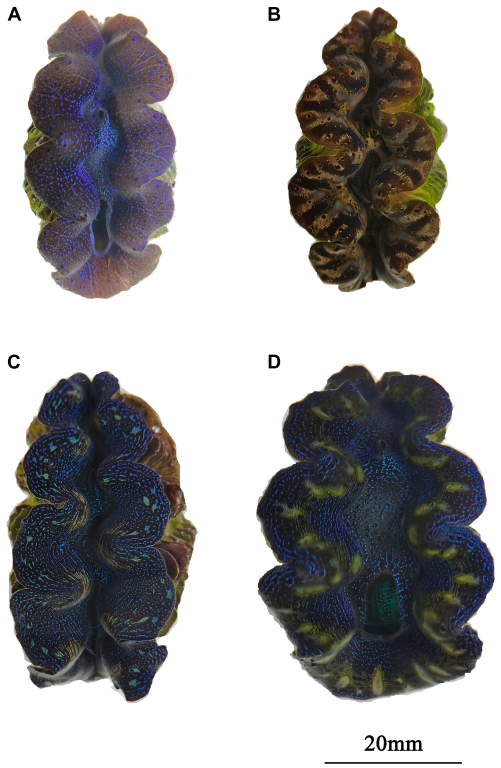

FIGURE 1 | Photos of progeny for boring giant clam *Tridacna crocea*. **(A)** BB progeny. **(B)** YY progeny. **(C)** BY Progeny. **(D)** YB Progeny. The bar indicates 30 mm, and it applies to all samples in **Figure 1**.

affected by the surrounding environment (Rawson and Feindel, 2012). In our study, the survival rate of reciprocal hybrids was higher than that of pure strains, which is manifested as a significant increase in the level of metamorphosis. The reciprocal hybrids have three iridocytes, while the blue and yellow-green strains have one or two iridocytes, which means that the hybrids have a higher degree of heterozygosity than other strains (Brake et al., 2004). The higher heterozygosity of the hybrid means higher physiological and immune levels, thus a higher survival rate than the progenies of two pure stains.

Inheritance of Mantle Color Patterns

The mantle coloration of giant clams can be divided into three stages: non-coloring period (days 0–60), coloring period (days 60–180), and stable expression period (>day 180) (Zhou et al., 2021). During the non-coloring period, no iridocytes occur, so the mantle color looks brown due to the accumulation of zooxanthellae. During the coloring period, iridocytes in the mantle begin to appear and increase in number, until they become visible to the naked eye about 6 months later. Interestingly, green iridocytes were found in early stage of both pure strains and reciprocal hybrids, suggesting that the green iridocyte may be ancestors of the others (Zhou et al., 2021).

After the early green iridocytes changed to blue (60–120 days), the mantle colors of the reciprocal hybrids were both blue during the coloring stage (120–180 days), which indicates that the expression of blue iridocytes is dominant in the mantle. The dominant expressions of phenotypic traits for progeny usually occur in the process of hybridization, which is likely to be an essential transitional phase in the overall life history of giant clams and may reflect the evolutionary strategy of nature. In some animals, particular color morphs may enhance camouflage, improve communication within species, and/or confer them a reproductive advantage (Korzan et al., 2008). Therefore, this staged dominant coloration is likely to be a camouflage, which may improve the survival rate of giant clam populations in wild coral reef areas (Fatherree, 2006; Neo et al., 2015).

During the stable expression period, the mantle color of two pure strains was 100% inherited, while all reciprocal hybrids have colorful colors in the mantle, which indicates that the genetic recombination of the mantle color has occurred. Genetic recombination usually occurs during meiosis, which involves the pairing of homologous chromosomes and is a key developmental program for gametogenesis (Brick et al., 2012). Novel phenotypic features are often formed in hybrid, which may accelerate the processes of species diversity via adaptive evolution (Abbott et al., 2013). In aquatic animals, the research on genetic recombination of body surface coloration is mainly focused on the ornamental carp (David et al., 2004). The mantle coloration of marine bivalves was only found on oysters and giant clams using hybridization or crossbreeding methods (Wang et al., 2015; Zhou et al., 2021). Furthermore, our results reveal that the colorful mantle of the giant clams may be caused by multiple random crossings between two individuals with different mantle colors during the reproductive stage.

Applicant Prospects

Giant clams are often covered with unique patterns and various colors. For a long time, why they look as fancy has been a mystery (Fatherree, 2006; Neo et al., 2015; Rossbach et al., 2021). In the aquarium market, the price of giant clam is partially determined according to the different mantle colors. For example, blue and purple giant clams are known as "amethyst," and their price is four to five times that of others varieties. The blue *Tridacna squamosa* can be sold for $180/ind, because the blue *T. squamosa* is an interspecific hybrid and is rare in nature. It is derived from female *T. squamosa* and male *Tridacna crocea*. Recently, these hybrids with heterosis have been mass produced, and they have the mantle color of *T. crocea* and shell of *T. squamosa* (Zhou et al., 2020).

With the use of mantle color as an indicator, it is important to carry out genetic breeding of giant clams, because the specific mantle color of individual clam can significantly increase

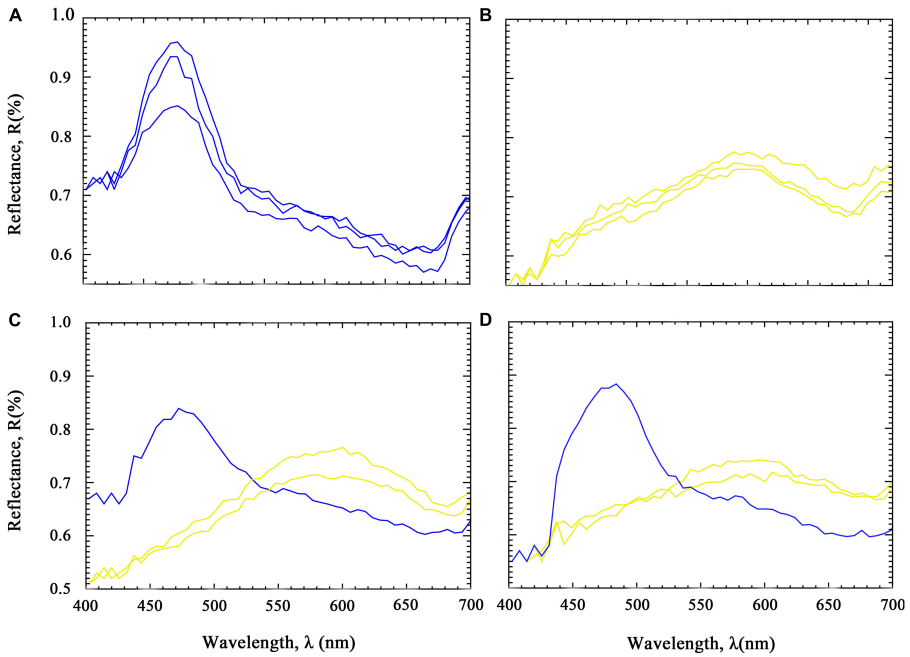

FIGURE 2 | Spectra from individual iridocytes from *Tridacna crocea*, corresponding to **Figure 1**. **(A)** BB progeny. **(B)** YY progeny. **(C)** BY Progeny. **(D)** YB Progeny. Each line indicates a single iridocyte's color with one main peak in the outer mantle.

economic value (Frias-Torres, 2017). According to our study, the mantle color lines can be produced by selective breeding, crossbreeding, and interspecific hybridization, which can then be used to breed new varieties of giant clams (Zhang et al., 2020a,b; Zhou et al., 2021). Therefore, this study provides a basic understanding and analysis of the mantle coloring inheritance of the boring giant clam and provides practice for the breeding of new giant clam varieties.

CONCLUSION

First, we found that the mantle color of blue and yellow-green giant clams can be stably inherited. Reciprocal hybrids express genetic recombination in the mantle color pattern and showed common dominant expression. This discovery demonstrates the formation and evolution of the mantle color polymorphism of *T. crocea* and provides a new direction for understanding the environmental adaptability and genetic breeding of the boring giant clams in the coral reef area.

DATA AVAILABILITY STATEMENT

The original contributions presented in the study are included in the article/supplementary materials, further inquiries can be directed to the corresponding author/s.

AUTHOR CONTRIBUTIONS

ZY and YHZ conceived and designed the experiments. ZZ, JL, HM, YQ, JW, XL, QL, and YL performed the experiments. YYZ, ZZ, GS, and YHZ analyzed the data. JW, YHZ, ZZ, JL, and ZY wrote the manuscript. All authors contributed to the article and approved the submitted version.

FUNDING

This work was supported by the Chinese Ministry of Science and Technology through the National Key Research and Development Program of China (2018YFD0901400 and 2020YFD0901100); the National Science Foundation of China (31872566, 31702340, and 32002387); Key Special Project for Introduced Talents Team of Southern Marine Science and Engineering Guangdong Laboratory (Guangzhou) (GML2019ZD0404); the China-ASEAN Maritime Cooperation Fund (CAMC-2018F); the Network Service Local Plan STS of the Chinese Academy of Sciences (KFJ-STS-QYZD-158); the Strategic Priority Research Program of the Chinese Academy of Sciences (XDA13020202); the Innovation Academy of South China Sea Ecology and Environmental Engineering, Chinese Academy of Sciences (ISEE2018PY01 and ISEE2018ZD02); the Open Foundation of the State Key Laboratory of Loess and Quaternary Geology (SKLLQG1813 and SKLLQG1918); the China Agricultural Shellfish Industry Technology System Project (CARS-49); and the Science and Technology Planning Project of Guangdong Province, China (2017B030314052).

ACKNOWLEDGMENTS

The authors would like to thank the editor and several reviewers for their assistance in the manuscript revision process.

REFERENCES

Abbott, R., Albach, D., Ansell, S., Arntzen, J. W., Baird, S. J., Bierne, N., et al. (2013). Hybridization and speciation. *J. Evol. Biol.* 26, 229–246. doi: 10.1111/j.1420-9101.2012.02599.x

Brake, J., Evans, F., and Langdon, C. (2004). Evidence for genetic control of pigmentation of shell and mantle edge in selected families of Pacific oysters, *Crassostrea gigas*. *Aquaculture* 229, 89–98. doi: 10.1016/S0044-8486(03)00325-9

Braley, R. D., Militz, T. A., and Southgate, P. C. (2018). Comparison of three hatchery culture methods for the giant clam *Tridacna noae*. *Aquaculture* 495, 881–887. doi: 10.1016/j.aquaculture.2018.05.044

Brick, K., Smagulova, F., Khil, P., Camerini-Otero, R. D., and Petukhova, G. V. (2012). Genetic recombination is directed away from functional genomic elements in mice. *Nature* 485, 642–645.

Cruz, P., and Ibarra, A. M. (1997). Larval growth and survival of two Catarina scallop (*Argopecten circularis*, Sowerby, 1835) populations and their reciprocal crosses. *J. Exp. Mar. Biol. Ecol.* 212, 95–110. doi: 10.1016/S0022-0981(96)02742-6

Cuthill, I. C., Allen, W. L., Arbuckle, K., Caspers, B., Chaplin, G., Hauber, M. E., et al. (2017). The biology of color. *Science* 357:eaan0221. doi: 10.1126/science.aan0221

David, L., Rothbard, S., Rubinstein, I., Katzman, H., Hulata, G., Hillel, J., et al. (2004). Aspects of red and black color inheritance in the Japanese ornamental (Koi) carp (*Cyprinus carpio L.*). *Aquaculture* 233, 129–147. doi: 10.1016/j.aquaculture.2003.10.033

Fatherree, J. (2006). Giant Clams in the Sea and the Aquarium: The Biology, Identification, and Aquarium Husbandry of Tridacnid Clams. Florida: Liquid Medium.

Frias-Torres, S. (2017). Captive bred, adult giant clams survive restoration in the wild in Seychelles, Indian Ocean. *Front. Mar. Sci.* 4:97. doi: 10.3389/fmars.2017.00097

Ghoshal, A., Eck, E., Gordon, M., and Morse, D. E. (2016). Wavelength-specific forward scattering of light by Bragg-reflective iridocytes in giant clams. *J. R. Soc. Interface* 13:20160285. doi: 10.1098/rsif.2016.0285

Griffiths, D. J., Winsor, H., and Luongvan, T. (1992). Iridophores in the mantle of giant clams. *Aust. J. Zool.* 40, 319–326. doi: 10.1071/ZO9920319

Holt, A. L., Vahidinia, S., Gagnon, Y. L., Morse, D. E., and Sweeney, A. M. (2014). Photosymbiotic giant clams are transformers of solar flux. *J. R. Soc. Interface* 11:20140678. doi: 10.1098/rsif.2014.0678

Kim, H. N., Vahidinia, S., Holt, A. L., Sweeney, A. M., and Yang, S. (2017). Geometric design of scalable forward scatterers for optimally efficient solar transformers. *Adv. Mater.* 29:1702922. doi: 10.1002/adma.201702922

Korzan, W. J., Robison, R. R., Zhao, S., and Fernald, R. D. (2008). Color change as a potential behavioral strategy. *Horm. Behav.* 54, 463–470. doi: 10.1016/j.yhbeh.2008.05.006

Long, C., Zhang, Y., Li, Y., Li, J., Zhou, Z., Qin, Y., et al. (2021). Effects of Symbiodinaaceae phylotypes in clades A-E on progeny performance of two giant clams (*Tridacna squamosa* and *T. crocea*) during early history life stages in the South China Sea. *Front. Mar. Sci.* 8:633761. doi: 10.3389/fmars.2021.633761

Ma, H., Gao, H., Zhang, Y., Qin, Y., Xiang, Z., Li, J., et al. (2021). Multiplex species-specific PCR identification of native giant clams in the South China Sea: a useful tool for application in giant clam stock management and forensic identification. *Aquaculture* 531:735991. doi: 10.1016/j.aquaculture.2020.735991

Mäthger, L. M., Senft, S. L., Gao, M., Karaveli, S., Bell, G. R., Zia, R., et al. (2013). Bright white scattering from protein spheres in color changing, flexible cuttlefish skin. *Adv. Funct. Mater.* 23, 3980–3989. doi: 10.1002/adfm.201203705

Mies, M. (2019). Evolution, diversity, distribution and the endangered future of the giant clam-Symbiodiniaceae association. *Coral Reef* 38, 1067–1084. doi: 10.1007/s00338-019-01857-x

Militz, T. A., Braley, R. D., and Southgate, P. C. (2017). Captive hybridization of the giant clams *Tridacna maxima* (Röding, 1798) and *Tridacna noae* (Röding, 1798). *J. Shellfish Res.* 36, 585–591. doi: 10.2983/035.036.0306

Militz, T. A., Braley, R. D., Schoeman, D. S., and Southgate, P. C. (2019). Larval and early juvenile culture of two giant clam (Tridacninae) hybrids. *Aquaculture* 500, 500–505. doi: 10.1016/j.aquaculture.2018.10.050

Neo, M. L., Eckman, W., Vicentuan, K., Teo, S. L.-M., and Todd, P. A. (2015). The ecological significance of giant clams in coral reef ecosystems. *Biol. Conserv.* 181, 111–123. doi: 10.1016/j.biocon.2014.11.004

Ozog, S. T. (2009). *Balancing Anti-Predation and Energetic Needs: Color Polymorphism in the Giant Clam Tridacna Maxima*. Berkeley, CA: University of California.

Rawson, P., and Feindel, S. (2012). Growth and survival for genetically improved lines of Eastern oysters (*Crassostrea virginica*) and interline hybrids in Maine, USA. *Aquaculture* 326, 61–67. doi: 10.1016/j.aquaculture.2011.11.030

Rossbach, S., Anton, A., and Duarte, C. M. (2021). Drivers of the abundance of *Tridacna spp*. giant clams in the Red Sea. *Front. Mar. Sci.* 7:592852. doi: 10.3389/fmars.2020.592852

Rossbach, S., Subedi, R. C., Ng, T. K., Ooi, B. S., and Duarte, C. M. (2020). Iridocytes mediate photonic cooperation between giant clams (Tridacninae) and their photosynthetic symbionts. *Front. Mar. Sci.* 7:465. doi: 10.3389/fmars.2020.00465

Wang, C., and Côté, J. (2012). Heterosis and combining abilities in growth and survival in sea scallops along the Atlantic coast of Canada. *J. Shellfish Res.* 31, 1145–1149. doi: 10.2983/035.031.0425

Wang, C., Liu, B., Li, J., Liu, S., Li, J., Hu, L., et al. (2011). Introduction of the Peruvian scallop and its hybridization with the bay scallop in China. *Aquaculture* 310, 380–387. doi: 10.1016/j.aquaculture.2010.11.014

Wang, Q., Li, Q., Cong, R., Kong, N., and Kong, L. (2015). Inheritance of mantle pigmentation in selected families of the Pacific oyster *Crassostrea gigas*. *Mar. Sci.* 39, 86–90.

You, W., Guo, Q., Fan, F., Ren, P., Luo, X., and Ke, C. (2015). Experimental hybridization and genetic identification of Pacific abalone *Haliotis discus haHHai* and green abalone *H. fulgens*. *Aquaculture* 448, 243–249. doi: 10.1016/j.aquaculture.2015.05.043

Zhang, H., Liu, X., Zhang, G., and Wang, C. (2007). Growth and survival of reciprocal crosses between two bay scallops, *Argopecten irradians concentricus* Say and *A. irradians irradians* Lamarck. *Aquaculture* 272, S88–S93. doi: 10.1016/j.aquaculture.2007.08.008

Zhang, Y., Li, J., Zhang, Y., Ma, H., Xiao, S., Xiang, Z., et al. (2017). Performance evaluation of reciprocal hybrids derived from the two brackish oysters, *Crassostrea hongkongensis* and *Crassostrea sikamea* in southern China. *Aquaculture* 473, 310–316. doi: 10.1016/j.aquaculture.2017.02.031

Zhang, Y., Ma, H., Li, X., Zhou, Z., Li, J., Wei, J., et al. (2020a). Analysis of inbreeding depression on performance traits of three giant clams (*Tridacna derasa*, *T. squamosa*, and *T. crocea*) in the South China Sea. *Aquaculture* 521:735023. doi: 10.1016/j.aquaculture.2020.735023

Zhang, Y., Zhou, Z., Qin, Y., Li, X., Ma, H., Wei, J., et al. (2020b). Phenotypic traits of two boring giant clam (*Tridacna crocea*) populations and their reciprocal hybrids in the South China Sea. *Aquaculture* 519:734890. doi: 10.1016/j.aquaculture.2019.734890

Zhou, Z., Li, J., Ma, H., Li, Y., Qin, Y., Wei, J., et al. (2021). The evaluation of culture performance and mantle coloration of two boring giant clam (Tridacna crocea) strains. *Aquaculture Rep.* 20:100646. doi: 10.1016/j.aqrep.2021.100646

Zhou, Z., Li, J., Ma, H., Qin, Y., Zhou, Y., Wei, J., et al. (2020). Artificial interspecific hybridization of two giant clams, *Tridacna squamosa* and *Tridacna crocea*, in the South China Sea. *Aquaculture* 515:734581. doi: 10.1016/j.aquaculture.2019.734581

Conflict of Interest: The authors declare that the research was conducted in the absence of any commercial or financial relationships that could be construed as a potential conflict of interest.